Electronic Supplementary Material (ESI) for Nanoscale.
This journal is © The Royal Society of Chemistry 2022

Supplementary Material

Cu-induced NiCu-P and NiCu-Pi with Multilayered Nanostructures as Highly Efficient Electrodes for Hydrogen Production via Urea Electrolysis

Xiao Xu,[1] Shan Ji,[2*] Hui Wang,[1] Xuyun Wang,[1**] Vladimir Linkov,[3] Peng Wang,[4] Lei Pan,[4] Guoqiang Wang,[4] Rongfang Wang[1***]

[1] State Key Laboratory Base for Eco-Chemical Engineering, College of Chemical Engineering, Qingdao University of Science and Technology, Qingdao, 266042, China

[2] College of Biological, Chemical Science and Engineering, Jiaxing University, Jiaxing, 314001, China

[3] South African Institute for Advanced Materials Chemistry, University of the Western Cape, Cape Town, 7535, South Africa

[4] Shandong Hydrogen Energy Co., Ltd, Weifang, 261000, China

Physical characterization

X-ray diffraction (XRD) was carried out on a Shimadzu XD-3A Instrument, which was fitted with a Cu-Kα radiation filter (λ = 0.15418 nm) and operated at 30 mA and 40 kV. A JEM-2000 FX JEOL microscope operated at 200 kV was used for recording transmission electron microscopy (TEM) and high angle annular dark-field scanning transmission electron microscopy (STEM) images as well as selected area electron diffraction (SAED) analysis. X-ray photoelectron spectra (XPS) were obtained on a VG Escalab210 Spectrometer with a Mg 300 W X-ray source. The reference value chosen for correcting the instrumental aberrations was depended on the binding energy of C 1s, which was 284.8 eV, and the number of scans for examined was 0.1 eV.

Electrochemical characterization

A three-electrode electrochemical cell linked with a potentiostat/galvanostat (CHI 760, CH Instruments) was applied to evaluate the HER, UOR and OER electrocatalytic properties. In this three-electrode cell, Hg/HgO and graphite rod were used as reference electrode (RE) and counter electrode (CE) respectively. For comparison, Pt/C and RuO_2 electrodes were also prepared by dispersing 16 mg the catalyst, 2 μL of polymer binder PTFE, 2 mg acetylene black in 300 μL isopropyl alcohol to form a homogenous slurry. After rolling into a slice and oven drying at 60℃, the mixture was pressed onto the 1 cm × 1 cm Ni foam under 20 MPa. 1.0 M KOH aqueous solution and 1.0 M KOH with 0.33 M urea aqueous solution were used as electrolyte for electrocatalytic testing. For convenience, the measured potential versus the reversible electrode (RHE) were converted according to the equation:

$$E_{RHE} = E_{Hg/HgO} + 0.059\ pH + 0.098 \quad (1)$$

Linear sweep voltammetry (LSV) were measured at a scan rate of 5 mV s^{-1}. The LSV curves were corrected for *iR* compensation (80%). Electrochemical impedance spectroscopy (EIS) spectra were measured at corresponding UOR and HER electrode potentials from 0.01 to 1,000,000 Hz with an amplitude of 5 mV. Moreover, a Nafion membrane was used for blocking bubble diffusion during the gas collection process by a classical drainage method in the three-electrode mode. The electrochemical surface area (ECSA) of the materials was derived from the double-layer capacitance (C_{dl}), which was measured by cyclic voltammetry (CV) in non-Faradaic regions under potentials ranging from -0.8 V to -0.7 V and from -0.1 V to -0 V vs Hg/HgO at scan rates from 20 mV s^{-1} to 120 mV s^{-1}. Currents at -0.75 V and -0.05 V were used to calculate C_{dl} and ECSA according to the following equations:

$$j = v \cdot C_{dl} \quad (2)$$

$$ECSA = C_{dl}/(C_s \times S) \quad (3)$$

Where j is the double-layer charging current density, v is the scan rate, C_s represents the specific electrode surface capacitance (μF cm^{-2}) and S is the working electrode area (cm^2). The value of C_s in an alkaline media was accepted to be 40 μF cm^{-2}.

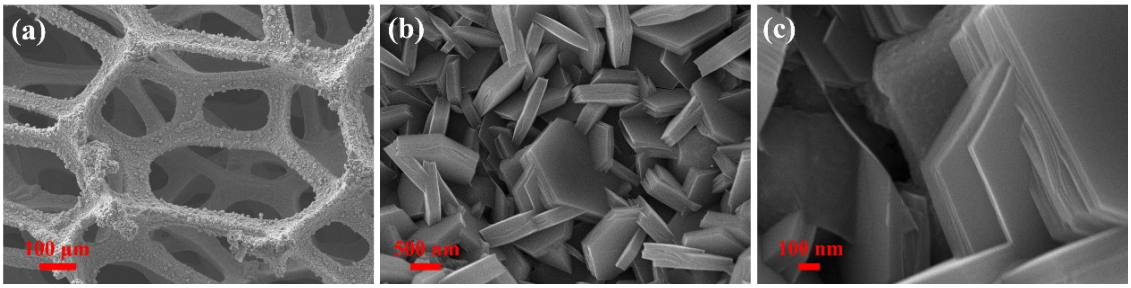

Figure S1. SEM images of NiCu-OH/NF-0.3.

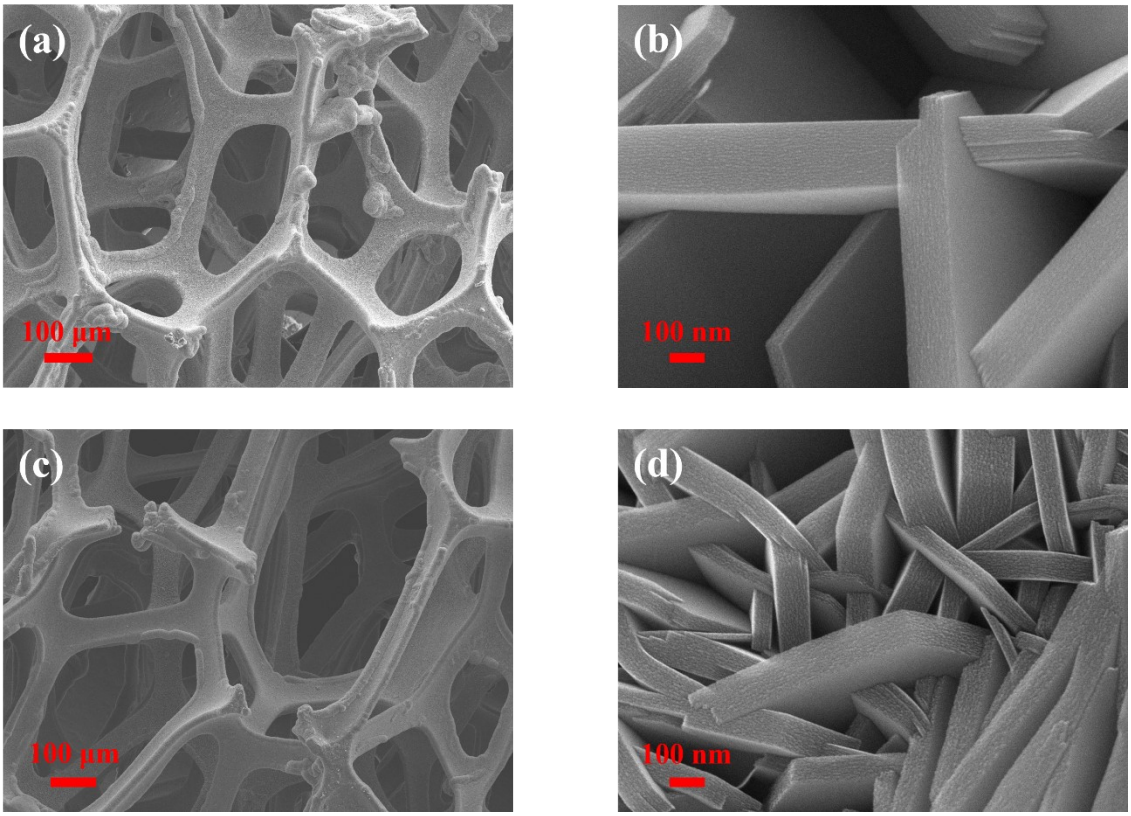

Figure S2. SEM images of Ni_2P/NF (a-b) and Ni-Pi/NF (c-d).

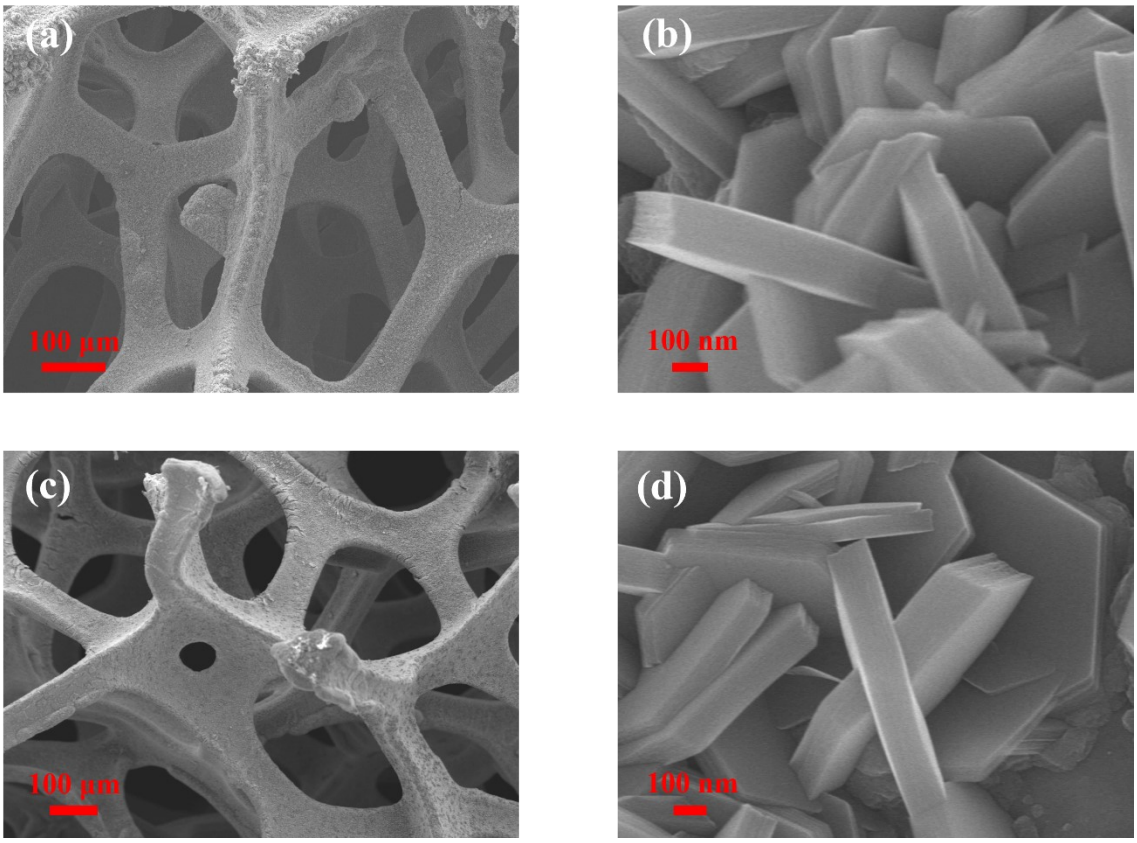

Figure S3. SEM images of NiCu-P/NF-0.1 (a-b) and NiCu-Pi/NF-0.1 (c-d).

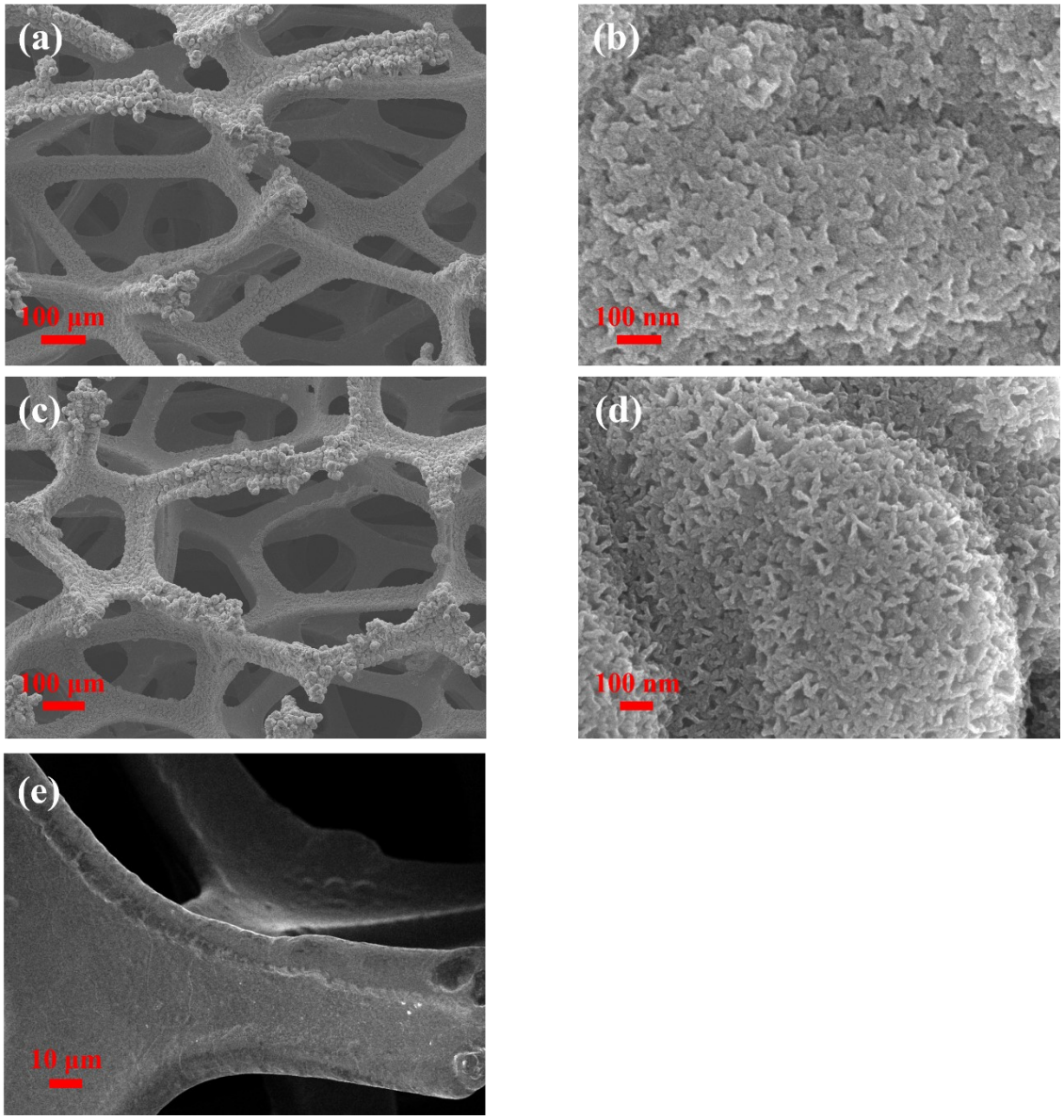

Figure S4. SEM images of NiCu-P/NF-0.5 (a-b); NiCu-Pi/NF-0.5 (c-d) and NF (e).

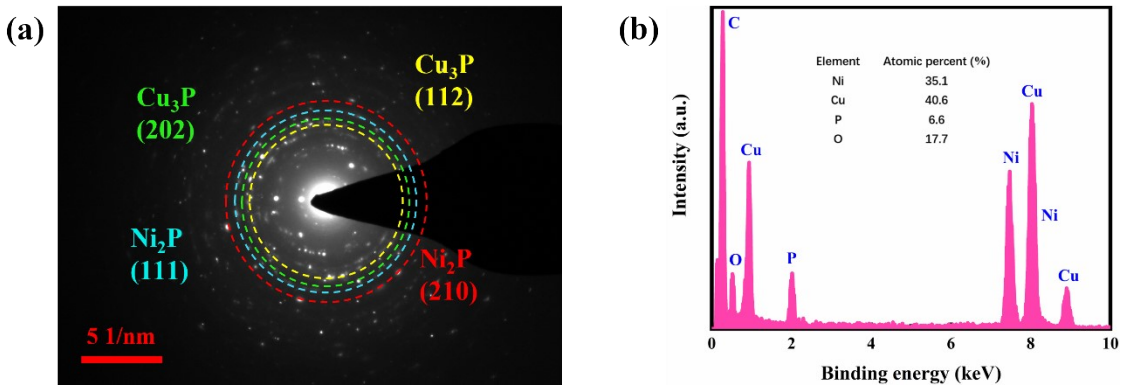

Figure S5. SEAD image (a) and EDX result (b) of NiCu-P/NF-0.3.

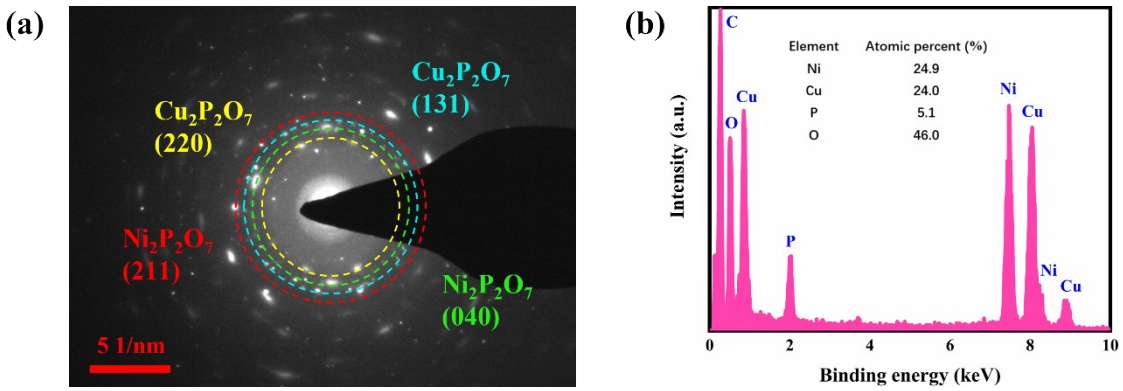

Figure S6. SEAD image (a) and EDX result (b) of NiCu-Pi/NF-0.3.

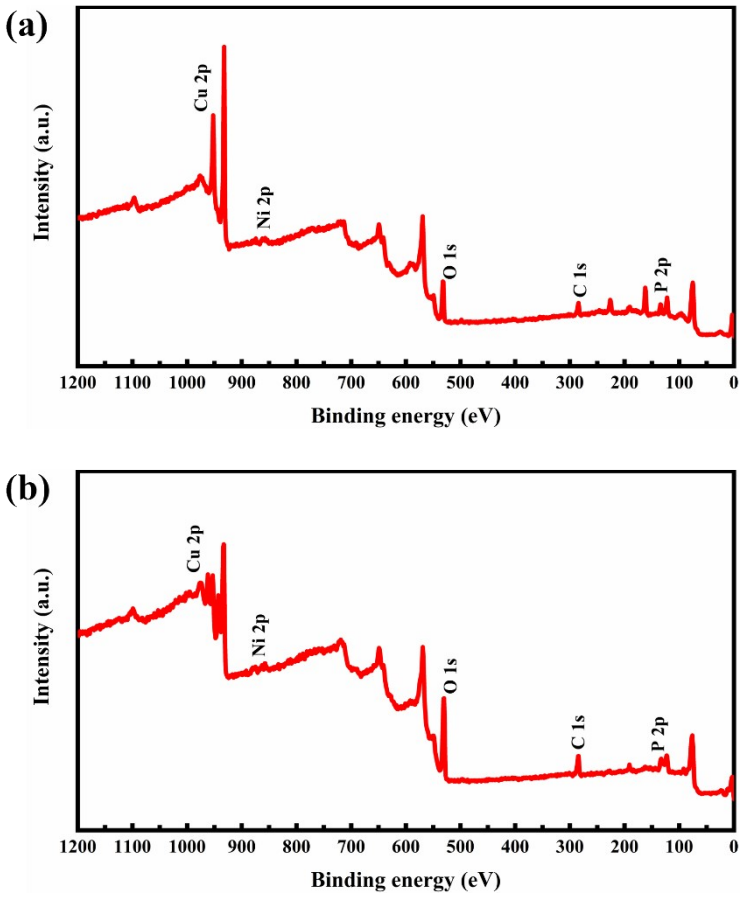

Figure S7. Survey XPS spectra of NiCu-P/NF-0.3 (a) and NiCu-Pi/NF-0.3 (b).

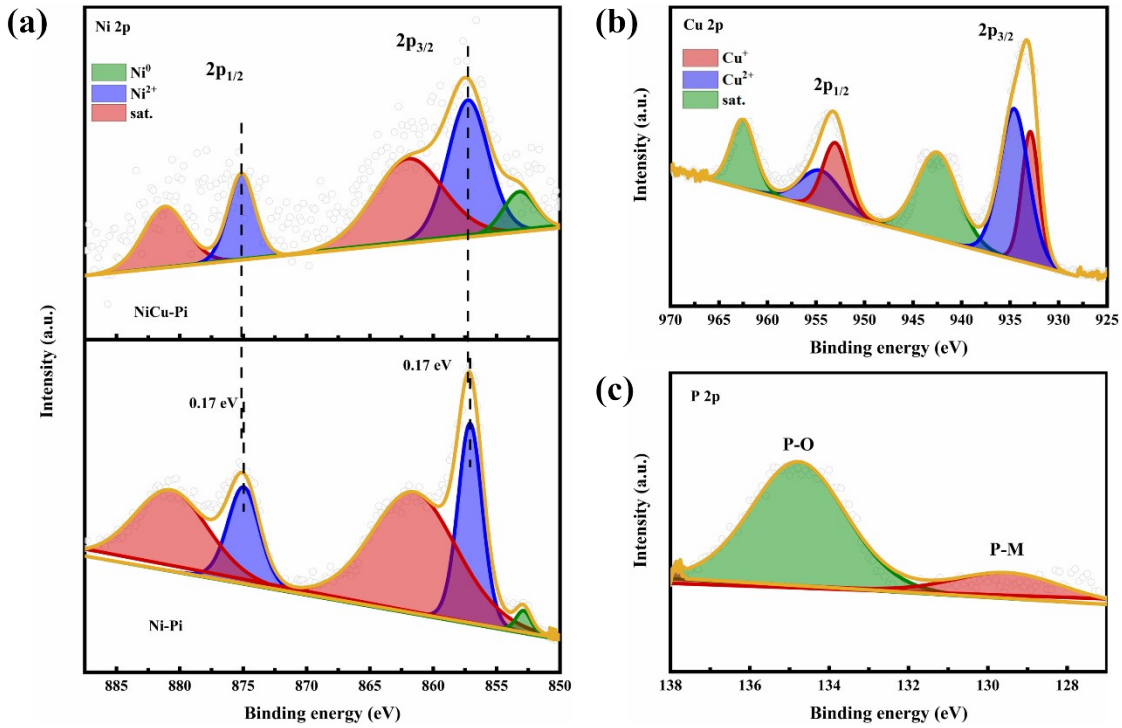

Figure S8. Ni 2p XPS of NiCu-Pi/NF-0.3 and Ni-Pi/NF (a); Cu 2p XPS (b) and P 2p XPS (c) of NiCu-Pi/NF-0.3.

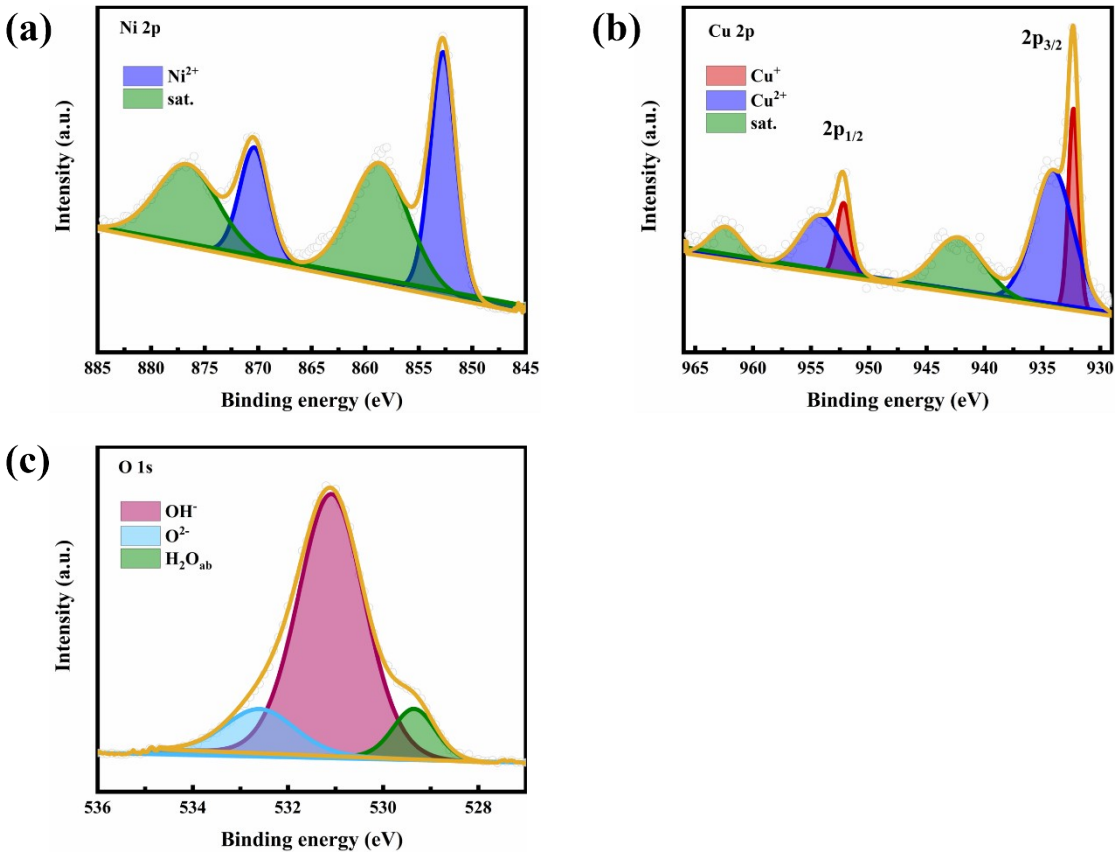

Figure S9. Ni 2p XPS (a), Cu 2p XPS (b) and P 2p XPS (c) of NiCu-OH/NF-0.3.

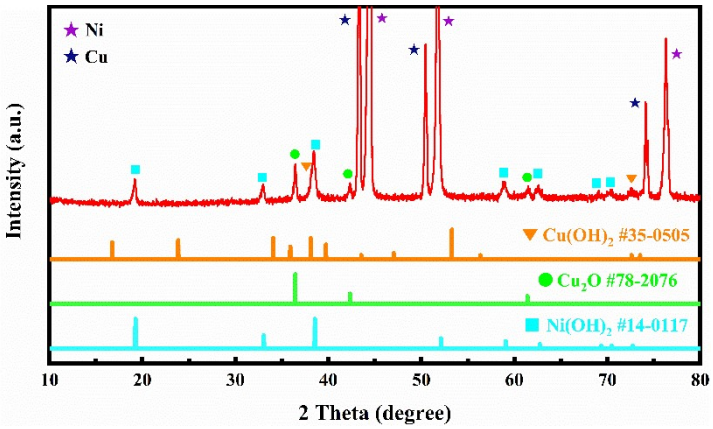

Figure S10. XRD pattern of NiCu-OH/NF-0.3

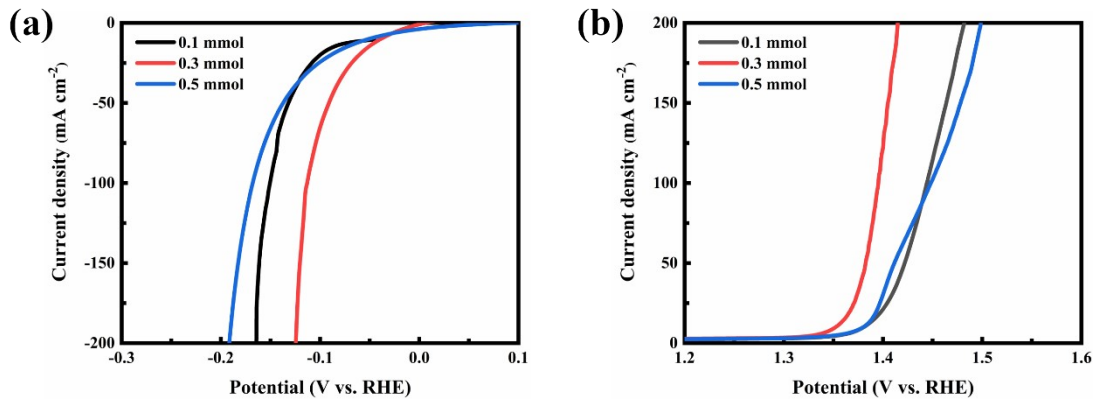

Figure S11. HER LSVs of NiCu-P/NF-0.1, NiCu-P/NF-0.3 and NiCu-P/NF-0.5 (a) and UOR LSVs of NiCu-Pi/NF-0.1, NiCu-Pi/NF-0.3 and NiCu-Pi/NF-0.5 (b).

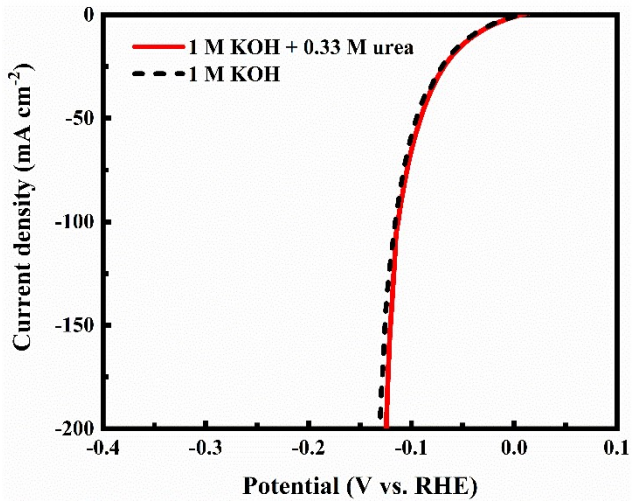

Figure S12. HER LSV in 1 M KOH with 0.33 M urea and 1 M KOH of NiCu-P/NF.

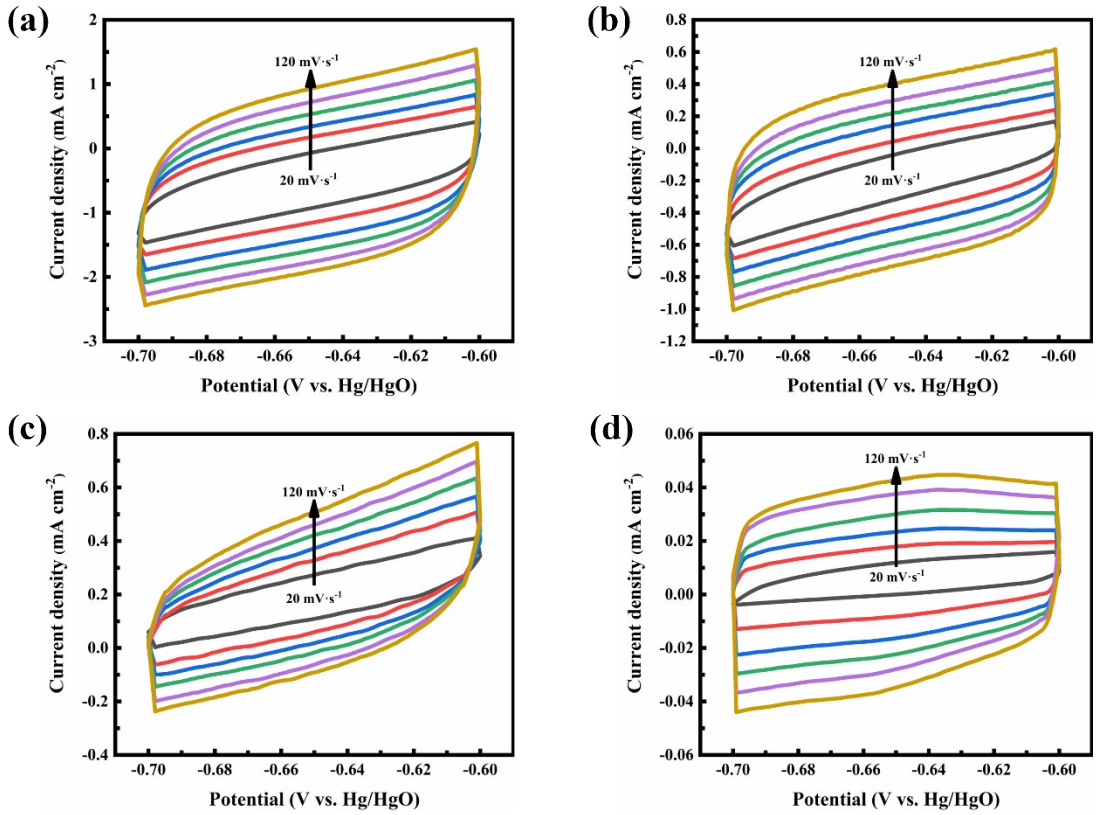

Figure S13. Cyclic Voltammetry plots at different scan rates (20 mV/s to 120 mV/s) of NiCu-P/NF (a), NiCu-OH/NF (b), Ni_2P/NF (c) and NF (d) for HER.

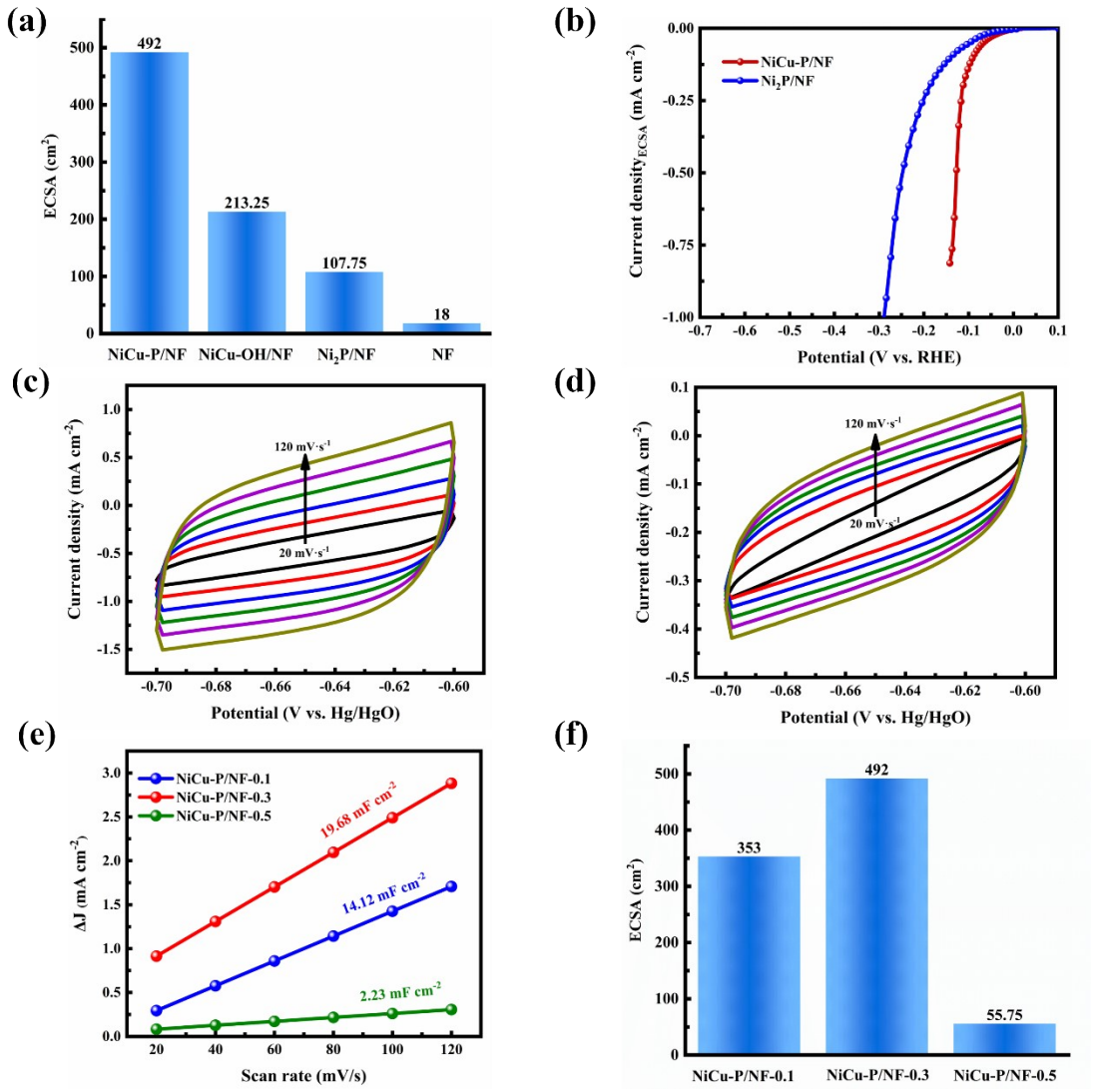

Figure S14. ECSA of NiCu-P/NF, NiCu-OH/NF, Ni_2P/NF and NF for HER (a) and ECSA normalized LSVs of HER (b); Cyclic Voltammetry plots at different scan rates (20 mV/s to 120 mV/s) of NiCu-P/NF-0.1 (c) and NiCu-P/NF-0.5 (d); ECSA of NiCu-P/NF-0.1, NiCu-P/NF-0.3 and NiCu-P/NF-0.5 for HER (e) and ECSA normalized LSVs of HER (f).

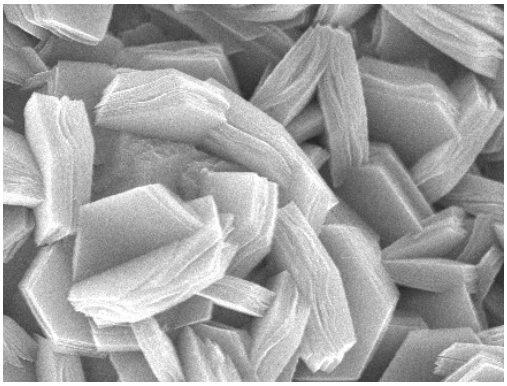

Figure S15. SEM image of NiCu-P/NF after HER stability testing.

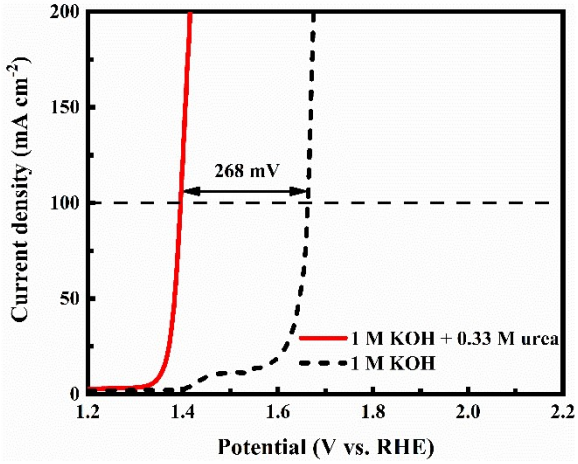

Figure S16. UOR LSV and OER LSV in 1 M KOH with 0.33 M urea and 1 M KOH of NiCu-Pi/NF.

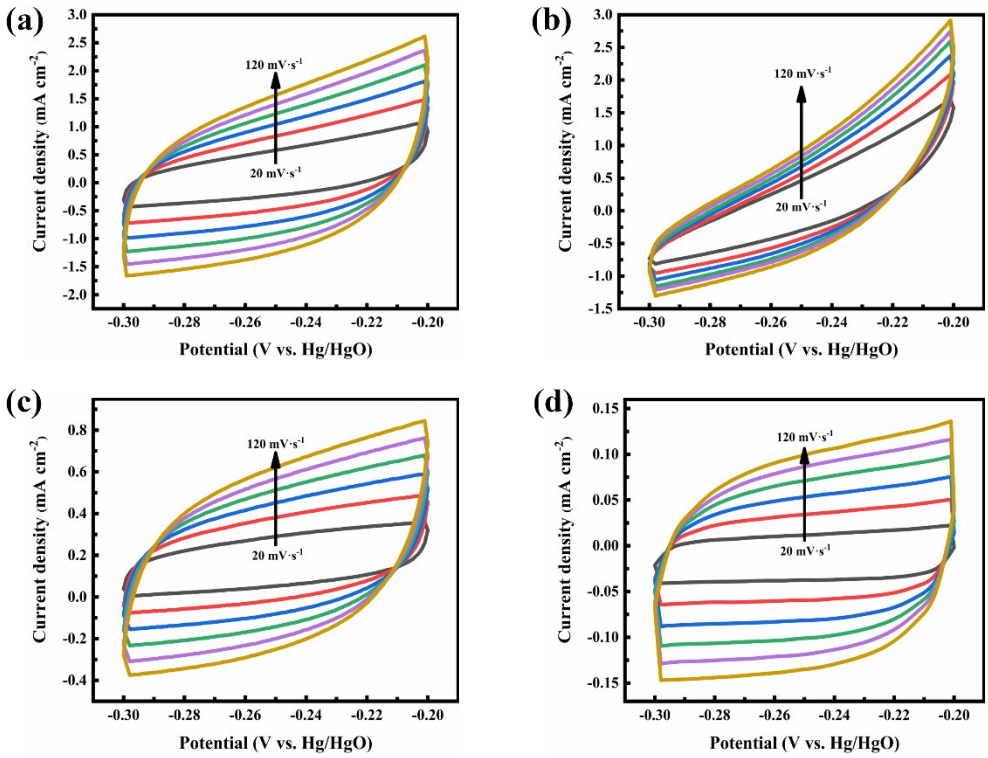

Figure S17. Cyclic Voltammetry plots at different scan rates (20 mV/s to 120 mV/s) of NiCu-Pi/NF (a), NiCu-OH/NF (b), Ni-Pi/NF (c) and NF (d) for UOR.

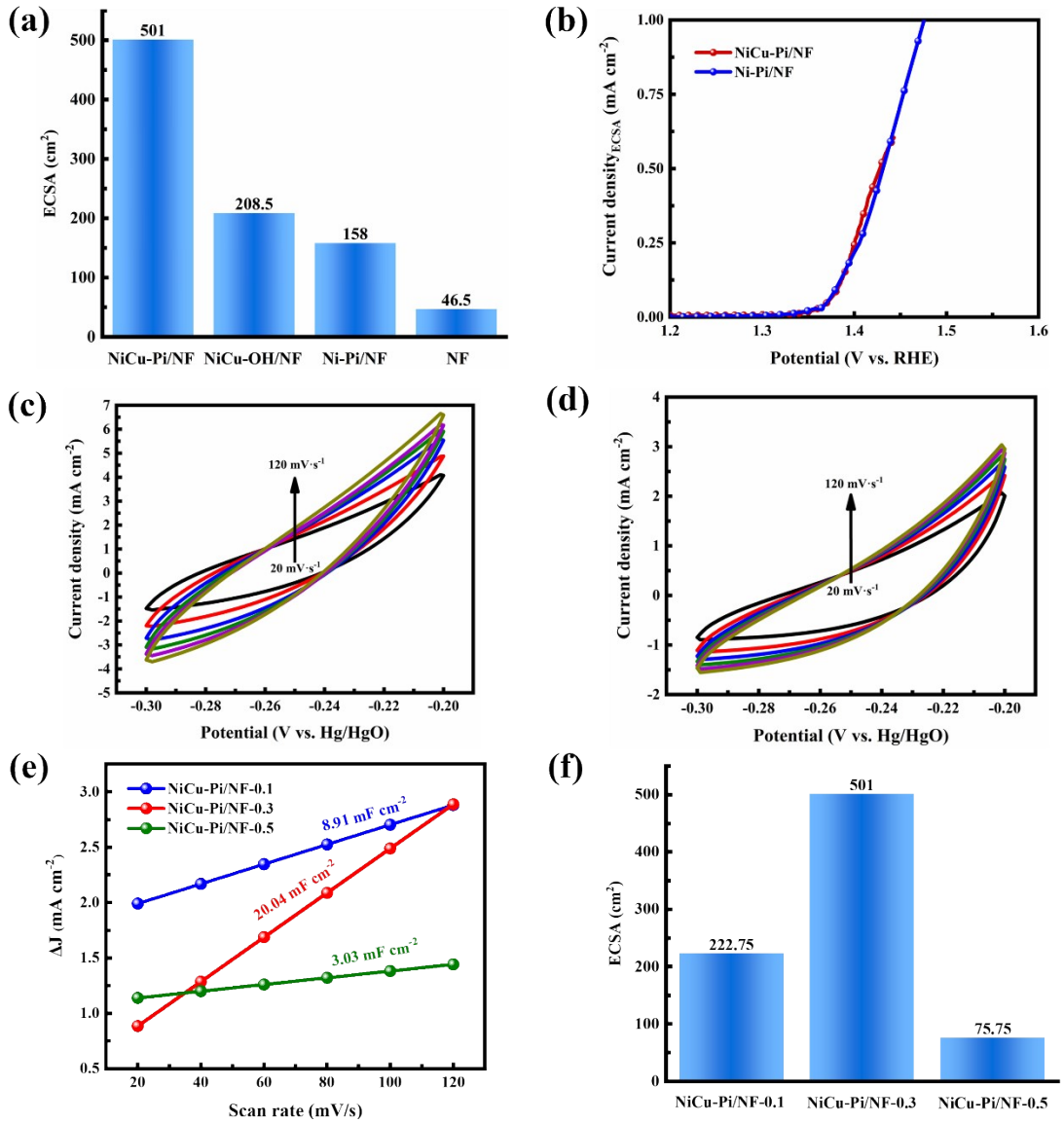

Figure S18. ECSA of NiCu-Pi/NF, NiCu-OH/NF, Ni-Pi/NF and NF for HER (a) and ECSA normalized LSVs of UOR.

Figure S19. SEM image of NiCu-Pi/NF after UOR stability testing.

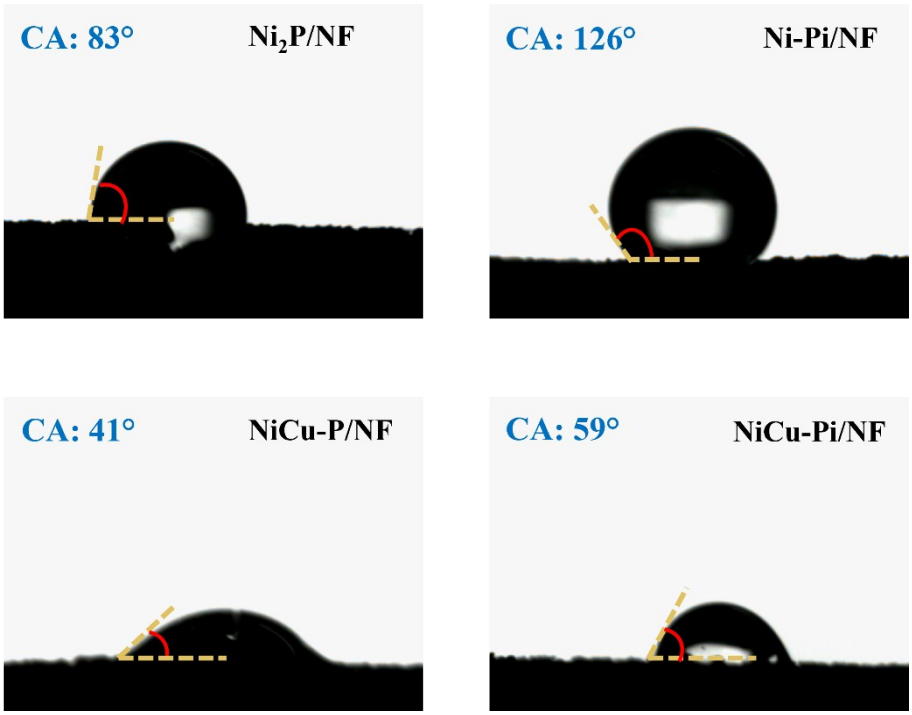

Figure S20. The contact angle images.

Table S1. ICP analysis data of metals in the as-prepared catalysts with different Cu dosages.

Materials	Loading amount (mg kg)		Atomic percentage	
	Ni	Cu	Ni	Cu
NiCu-P/NF-0.1	960886.2	31539.8	96.0886%	3.1540%
NiCu-P/NF-0.3	922250.5	73771.8	92.2251%	7.3772%
NiCu-P/NF-0.5	847836.7	139726.9	84.7837%	13.9727%

Table S2. The relative peak area of the orbital peaks.

Element	Materials	Relative peak area			
Ni	NiCu-P/NF	$2p_{1/2}$ Ni^{2+}-62%	$2p_{1/2}$ Ni^{0}-38%	$2p_{3/2}$ Ni^{2+}-62%	$2p_{3/2}$ Ni^{0}-38%
	NiCu-Pi/NF	/		$2p_{3/2}$ Ni^{2+}-81%	$2p_{3/2}$ Ni^{0}-19%
	NiCu-OH/NF	/			
Cu	NiCu-P/NF	$2p_{1/2}$ Cu^{2+}-54%	$2p_{1/2}$ Cu^{+}-46%	$2p_{3/2}$ Cu^{2+}-31%	$2p_{3/2}$ Cu^{+}-69%
	NiCu-Pi/NF	$2p_{1/2}$ Cu^{2+}-53%	$2p_{1/2}$ Cu^{+}-47%	$2p_{3/2}$ Cu^{2+}-66%	$2p_{3/2}$ Cu^{+}-34%
	NiCu-OH/NF	$2p_{1/2}$ Cu^{2+}-70%	$2p_{1/2}$ Cu^{+}-30%	$2p_{3/2}$ Cu^{2+}-73%	$2p_{3/2}$ Cu^{+}-27%
P	NiCu-P/NF	P-M -18%		P-O -82%	
	NiCu-Pi/NF	P-M -15%		P-O -85%	
O	NiCu-OH/NF	OH^{-} -80%		O^{2-} -13%	H_2O_{ab} -7%

Table S3. EIS resistance (Ω) fitting values.

Materials	UOR		HER	
	R_s	R_{ct}	R_s	R_{ct}
NF	0.98	47.24	0.85	49.51
NiCu-OH/NF	0.70	24.81	0.99	16.65
Ni_2P/NF	/		1.04	18.81
NiCu-P/NF	/		0.72	5.79
Ni-Pi/NF	1.08	8.98	/	
NiCu-Pi/NF	0.63	5.95	/	

Table S4. Conductivity and square resistance of different materials.

Materials	Square resistance (mΩ·mm)	Conductivity (KS/mm)
NF	2.87	0.35
NiCu-OH/NF	2.33	0.43
Ni_2P/NF	1.92	0.52
NiCu-P/NF	1.64	0.61
Ni-Pi/NF	2.12	0.47
NiCu-Pi/NF	1.78	0.56

Table S5. Cell voltage of different Ni-based electrodes found in recently reported literature.

Electrode	Morphology	Electrolyte	Cell voltage (V)	Ref.
NiCu-P/NF and NiCu-Pi/NF	Multilayer Structure	1 M KOH+0.33 M Urea	1.410 (10 mA cm^{-2}) 1.514 (50 mA cm^{-2}) 1.568 (100 mA cm^{-2})	This work
NiCoB@C	Alloy	1 M KOH+0.33 M Urea	1.62 (100 mA cm^{-2})	[1]
$Ni(OH)_2$@NF	Core-shell	1 M KOH+0.3 M Urea	1.45 (50 mA cm^{-2})	[2]
Co-$Ni(OH)_2$/NF	Nanoparticle	1 M KOH+0.5 M Urea	1.63 (50 mA cm^{-2})	[3]
Ni-Co_9S_8/CC	Nanosheet	1 M KOH+0.33 M Urea	1.52 (10 mA cm^{-2})	[4]
Ni_2P/$Ni_{0.96}S$/NF	Microsphere	1 M KOH+0.5 M Urea	1.453 (10 mA cm^{-2})	[5]
Ni_3N/NF	Nanosheet	1 M KOH+0.5 M Urea	1.51 (100 mA cm^{-2})	[6]
NiF_3/Ni_2P@CC	Nanoparticle	1 M KOH+0.33 M Urea	1.54 (10 mA cm^{-2})	[7]
V-$FeNi_3N$/Ni_3N	Nanosheet	1 M KOH+0.33 M Urea	1.46 (10 mA cm^{-2})	[8]
NF/PPy-Ni_3S_2	Nanowire	1 M KOH+0.33 M Urea	1.5 (20 mA cm^{-2})	[9]
NiS/MoS_2/NF	Nanosheet	1 M KOH+0.5 M Urea	1.48 (10 mA cm^{-2})	[10]
S-Co_2P@Ni_2P	Core-shell	\	1.43 (10 mA cm^{-2})	[11]
NiO/Ni_2P/NF	Nanosheet	1 M KOH+0.33 M Urea	1.559 (50 mA cm^{-2})	[12]
Ni_3S_2-NiS/NF	Nanorod	1 M KOH+0.5 M Urea	1.54 (50 mA cm^{-2})	[13]
NiFeMo/NF	Film	1 M KOH+0.33 M Urea	1.46 (10 mA cm^{-2})	[14]
NiMoSe/NF	Nanosphere	1 M KOH+0.33 M Urea	1.44 (10 mA cm^{-2})	[15]

References

1. B. Kim, G. Das, J. Kim, H. H. Yoon and D. H. Lee, *J. Colloid Interface Sci.*, 2021, **601**, 317-325.
2. L. Xia, Y. Liao, Y. Qing, H. Xu, Z. Gao, W. Li and Y. Wu, *ACS Appl. Energ. Mater.*, 2020, **3**, 2996-3004.
3. C. B. Sun, M. W. Guo, S. S. Siwal and Q. B. Zhang, *J. Catal.*, 2020, **381**, 454-461.
4. P. Hao, W. Zhu, L. Li, J. Tian, J. Xie, F. Lei, G. Cui, Y. Zhang and B. Tang, *Electrochim. Acta*, 2020, **338**, 135883.
5. M. He, C. Feng, T. Liao, S. Hu, H. Wu and Z. Sun, *ACS Appl. Mater. Interfaces*, 2020, **12**, 2225-2233.
6. Z. Zhao, J. Zhao, H. Wang, X. Li, L. Yang, Z. Zhao, X. Liu, Y. Liu, P. Liu and Z. Cai, *Int. J. Hydrogen Energ.*, 2020, **45**, 14199-14207.
7. K. Wang, W. Huang, Q. Cao, Y. Zhao, X. Sun, R. Ding, W. Lin, E. Liu and P. Gao, *Chem. Eng. J.*, 2022, **427**, 130865.
8. J. Wang, Y. Sun, Y. Qi and C. Wang, *ACS Appl. Mater. Interfaces*, 2021, **13**, 57392-57402.
9. Y. Zhang, Y. Qiu, Y. Wang, B. Li, Y. Zhang, Z. Ma and S. Liu, *ACS Appl. Mater. Interfaces*, 2021, **13**, 3937-3948.
10. C. Gu, G. Zhou, J. Yang, H. Pang, M. Zhang, Q. Zhao, X. Gu, S. Tian, J. Zhang, L. Xu and Y. Tang, *Chem. Eng. J.*, 2022, **443**, 136321.
11. W. Yuan, T. Jiang, X. Fang, Y. Fan, S. Qian, Y. Gao, N. Cheng, H. Xue and J. Tian, *Chem. Eng. J.*, 2022, **439**, 135743.
12. X. Xu, S. Ji, H. Wang, X. Wang, V. Linkov and R. Wang, *J. Colloid Interface Sci.*, 2022, **615**, 163-172.
13. Q. Zhao, C. Meng, D. Kong, Y. Wang, H. Hu, X. Chen, Y. Han, X. Chen, Y. Zhou, M. Lin and M. Wu, *ACS Sustain. Chem. Eng.*, 2021, **9**, 15582-15590.
14. Z. Lv, Z. Li, X. Tan, Z. Li, R. Wang, M. Wen, X. Liu, G. Wang, G. Xie and L. Jiang, *Appl. Surf. Sci.*, 2021, **552**, 149514.
15. H. Wang, X. Jiao, W. Zeng, Y. Zhang and Y. Jiao, *Int. J. Hydrogen Energ.*, 2021, **46**, 37792-37801.